

Analysis of coherent structures and atmosphere-canopy coupling strength during the CABINEX field campaign

A. L. Steiner¹, S. N. Pressley², A. Botros³, E. Jones⁴, S. H. Chung², and S. L. Edburg⁵

¹Department of Atmospheric, Oceanic and Space Sciences, University of Michigan, Ann Arbor, MI, USA

²Department of Civil and Environmental Engineering, Washington State University, Pullman, WA, USA

³Department of Neuroscience, University of California, Los Angeles, CA, USA

⁴Franklin W. Olin College of Engineering, Needham, MA, USA

⁵Department of Geography, University of Idaho, Moscow, ID, USA

Received: 20 June 2011 – Published in Atmos. Chem. Phys. Discuss.: 26 July 2011

Revised: 4 November 2011 – Accepted: 9 November 2011 – Published: 1 December 2011

Abstract. Intermittent coherent structures can be responsible for a large fraction of the exchange between a forest canopy and the atmosphere. Quantifying their contribution to momentum and heat fluxes is necessary to interpret measurements of trace gases and aerosols within and above forest canopies. The primary objective of the Community Atmosphere-Biosphere Interactions Experiment (CABINEX) field campaign (10 July 2009 to 9 August 2009) was to study the chemistry of volatile organic compounds (VOC) within and above a forest canopy. In this manuscript we provide an analysis of coherent structures and canopy-atmosphere exchange during CABINEX to support in-canopy gradient measurements of VOC. We quantify the number and duration of coherent structure events and their percent contribution to momentum and heat fluxes with two methods: (1) quadrant-hole analysis, and (2) wavelet analysis. Despite differences in the duration and number of events, both methods predict that coherent structures contribute 40–50 % to momentum fluxes and 44–65 % to heat fluxes during the CABINEX campaign. Contributions associated with coherent structures are slightly greater under stable atmospheric conditions. By comparing heat fluxes within and above the canopy, we determine the degree of coupling between upper canopy and atmosphere, and find that they are coupled the majority of the time. Uncoupled canopy-atmosphere events occur in the early morning (4–8 a.m. local time) approximately 30 % of the time. This study con-

firms that coherent structures contribute significantly to the exchange of heat and momentum between the canopy and atmosphere at the CABINEX site, and indicates the need to include these transport processes when studying the mixing and chemical reactions of trace gases and aerosols between a forest canopy and the atmosphere.

1 Introduction

Turbulent mixing is the fundamental driver in the exchange of mass, momentum and scalars between a forest canopy and the atmosphere (Finnigan et al., 2009; Harman and Finnigan, 2008). Quantifying these turbulent processes is necessary to understand the surface energy budget (Oncley et al., 2007), the global carbon budget (Law et al., 2002) and the fate of reactive trace gas species (Holzinger et al., 2005; Sörgel et al., 2011). These vertical motions are particularly relevant for atmospheric chemistry, where highly reactive gases and aerosols may have reaction time scales on the same order of magnitude as transport time scales (Dlugi et al., 2010; Fuentes et al., 2007).

Characterizing exchange between tall vegetation canopies and the atmosphere is complex because the roughness elements generate intermittent coherent structures (Finnigan, 2000). Coherent structures are defined as a distinct pattern of organized turbulence with length scales on the order of the canopy height. They typically result from hydrodynamic instabilities caused by large differences in horizontal wind speeds (wind shear) near the top of the canopy (Finnigan et al., 2009) and are thought to be the main driver of local-scale



Correspondence to: A. L. Steiner
(alsteiner@umich.edu)

counter-gradient flow (Raupach and Thom, 1981). Two primary types of exchange motion can occur: (1) A relatively slow “burst” or ejection of air from within the canopy to the atmosphere (representing upward motion) and (2) a relatively fast downward motion, or “sweep”, that brings air from the atmosphere into the forest canopy. Coherent structures have been shown to dominate the exchange between a forest canopy and the atmosphere (Brunet and Irvine, 2000; Collineau and Brunet, 1993a; Raupach et al., 1996). Previous studies indicate that coherent structures are more effective at transmitting scalars than momentum (Thomas and Foken, 2007) and can account for 40–87 % of the total amount of sensible heat fluxes in forested regions (Barthlott et al., 2007). This suggests coherent structures could be an important factor in the analysis of chemical concentration gradients and fluxes, as measured gradients are often used to interpret chemical and physical processes of the forest canopy e.g., (Holzinger et al., 2005; Rizzo et al., 2010; Wolfe et al., 2011).

Several techniques have been developed to isolate coherent structure events from the background fluctuations in momentum and energy fluxes including (1) quadrant-hole (Q-H) analysis (Bergstrom and Hogstrom, 1989; Finnigan, 1979; Lu and Willmarth, 1973; Raupach, 1981; Shaw et al., 1983) and (2) wavelet transform analysis (Collineau and Brunet, 1993a; Gao et al., 1989; Farge, 1992). Q-H analysis is a relatively simple approach that places the fluctuating components of the horizontal and vertical velocities into quadrants based on whether they are positive or negative, and then uses an exclusion region or “hole-size” to eliminate small-scale motion and isolate stronger events. Wavelet transform analysis is a more complex approach that typically uses the temperature time series and a wavelet as an integration kernel to define a continuous wavelet transform of the time series to detect events. This method identifies changes in power at specific points within a time series, which can represent the presence of a coherent structure.

While coherent structures have been identified as significant in the micrometeorological community, very few one-dimensional or three-dimensional atmospheric models of canopy-atmosphere exchange directly simulate the contribution of coherent structures to vertical mixing. The most simplistic vertical mixing parameterizations rely on K -theory, which assumes turbulent motion is analogous to molecular diffusion and relates a vertical flux to a vertical gradient through the eddy diffusivity parameter (K) (Foken, 2008). More complex models build on this approach but use higher order turbulence closure to represent turbulent fluxes (e.g., Yamada and Mellor, 1975; Katul et al., 2004). However, to fully capture coherent structures, a simulation technique such as large-eddy simulation (LES) is required. LES solves the spatially filtered Navier-Stokes equations and can directly simulate coherent structures in atmospheric boundary layer flows (Moeng, 1984; Patton et al., 2001).

In this paper, we estimate and evaluate the contribution of coherent structures to vertical fluxes of heat and momentum within and above a forest canopy during a recent field campaign in the summer of 2009 at the University of Michigan Biological Station (UMBS). The Community Atmosphere-Biosphere Interactions Experiment (CABINEX) field study was designed to elucidate the role of biogenic volatile organic compounds (VOC) and atmospheric oxidation within the canopy. As part of CABINEX, physical and chemical measurements were conducted at multiple heights within the forest canopy. While previous studies have evaluated turbulence at the UMBS AmeriFlux site (e.g., Su et al., 2008; Villani et al., 2003), a detailed analysis of coherent structures at the same spatial location and time of CABINEX chemical measurements is required for interpretation of chemical gradient measurements and other flux measurements at the UMBS facility. This description of canopy-atmosphere coupling can be useful in conjunction with chemical gradient measurements (e.g. Sörgel et al., 2011) and modeling to understand the role of mixing in atmospheric chemistry studies. The UMBS experimental facility has a broad research community using the site for a wide variety of flux measurements, ranging from biogenic VOC to carbon dioxide and nitrogen fluxes. Further, this work can be useful for scientists studying atmospheric chemistry at other similar ecosystems. The goal of this paper is to identify coherent structure contributions to mixing in the forest canopy and highlight time periods when the canopy is coupled to the atmosphere. The use of two coherent detection methods provides a comparison of techniques that is infrequently implemented in existing literature (Thomas and Foken, 2007).

2 Site and meteorological data description

2.1 Site and field campaign description

The UMBS site is located on approximately 4000 hectares of mixed deciduous forest in northern Michigan near the city of Pellston (45°35' N, 84°42' W). The stand age is approximately 90 years old and has a mean canopy height of 22.5 m (Fig. 1; see Carroll et al. (2001) for a full site description). UMBS has three large atmospheric flux towers, including the Forest Accelerated Succession Experiment (FASET) tower installed in the fall of 2006 (Nietz, 2010), an AmeriFlux tower established in June 1998 (Baldocchi et al., 2001), and a tower for dedicated atmospheric chemistry studies established in 1996 during the Program for Research on Oxidants: PHotochemistry, Emissions, and Transport (PROPHET) (Carroll et al., 2001). This study utilizes data collected at the PROPHET tower, located approximately 130 m southeast of the AmeriFlux tower. The 2009 CABINEX field campaign was an atmospheric chemistry experiment with a focus on measuring in-canopy oxidation of biogenic VOC species and formation of aerosols. The PROPHET

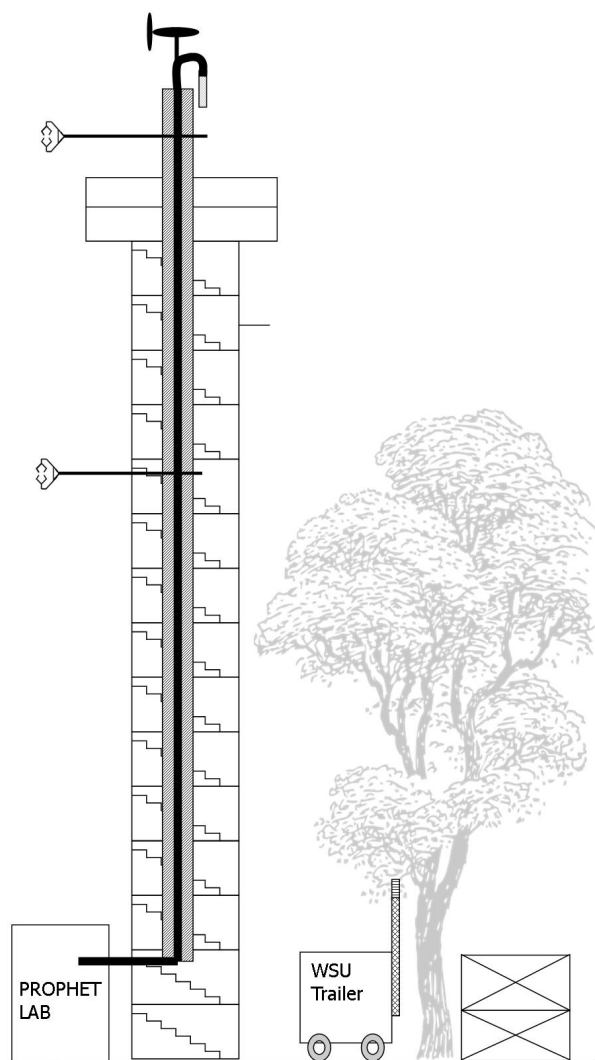


Fig. 1. University of Michigan Biological Station (UMBS) PROPHET tower schematic as configured for CABINEX 2009. Two sonic anemometers were used for this study: “top” at 34 m (1.5 canopy height) and “mid” at 20.6 m (0.92 canopy height).

tower (Fig. 1) was equipped with physical and chemical instrumentation extending above the tower platform (36.4 m), on the tower platform (31.2 m), in the mid-canopy (20.4 m) and near the forest floor (5 m) (see other manuscripts in this ACP special issue for more detail on specific chemical measurements). Data for this paper were collected using two high frequency sonic anemometers (CSAT-3, Campbell Scientific Instruments) located at the top of the tower, 1.5 times the canopy height (h) (34 m; 1.5 h) and within the upper portion of the canopy (20.6 m; 0.92 h). At the commencement of the campaign, sonic locations were selected to be above the canopy and in the upper portion of the canopy based on the CABINEX campaign goals concerned with whole-canopy processing of chemical compounds and aerosols. The sonic

locations are not candidates for investigating the role of sub-canopy turbulence, and discerning the role of the sub-canopy from the upper canopy on chemical processing is an area of future study. In the following work, we discuss the canopy-atmosphere exchange in the upper portion of the canopy.

2.2 Sonic anemometer data processing

Data from sonic anemometers were collected continuously at a rate of 10 Hz from 10 July–8 August 2009. Raw data for each anemometer includes the three velocity components (defined here as streamwise (u), cross-streamwise (v), and vertical (w)), and temperature (T). Additionally, 10 Hz CO_2 and H_2O concentrations were collected at the top sonic location using an open path infrared gas analyzer (IRGA, Licor 7500a). High frequency data (10 Hz) are pre-processed in 30-min periods (18 000 data points per file) as follows:

1. Data points outside a specified range of the 30-min mean (\pm five standard deviations) are classified as noise, removed, and replaced with the 30-min mean. These are likely due to instrument noise or other external factors.
2. Coordinate rotation is applied, assuming a negligible 30-min mean vertical velocity and a rotation of the streamwise axis into the mean wind direction (Foken, 2008).

After pre-processing, Reynolds decomposition is applied to temperature and three wind components, with each variable separated into its mean (30-min average) component (u) and the fluctuating component (u'). Fluxes are calculated for each 30-min time period as an average product of the 10 Hz fluctuation components (e.g. $\overline{u'w'}$ for the kinematic momentum flux and $\overline{w'T'}$ for kinematic heat flux). The Obukhov length (L) is calculated to determine the atmospheric stability for each 30-min time period as:

$$L = -\frac{u_*^3}{k \frac{g}{T} \overline{w'T'}} \quad (1)$$

where u_* is the friction velocity (m s^{-1}), k is the von Karman constant, g is the gravitational constant (9.81 m s^{-2}), \overline{T} is the average temperature, and $\overline{w'T'}$ the kinematic heat flux. L classifies 30-min time periods as unstable ($L < 0$), stable ($L \geq 0$), and neutral ($|L| \geq 1000$, where we interpret absolute values greater than 1000 as approaching infinity).

2.3 Additional data filters for coherent structure analysis

Approximately 30 days of sonic anemometer data (10 July–8 August 2009) are analyzed (1410 possible 30-min periods), with specific 30-min time periods removed from the analysis due to: (1) missing data: incomplete records from either

anemometer (40 30-min periods or 2.8 % of the total), (2) rain events: any detected rain at the nearby UMBS AmeriFlux tower (67 30-min periods, 4.8 %), (3) wind speeds: less than 1 m s^{-1} measured at the upper anemometer to remove weak wind conditions (99 30-min periods, 7.0 %) and 4) wind direction: winds measured at the upper sonic from directions coming through the tower could be subject to interference (winds between 125 and 165 degrees with the sonic oriented towards 325 degrees) (103 periods, 7.3 %). After applying these four filters, 1152 30-min time periods (82 % of total) are available for further analysis.

3 Methods

We use two different methods to detect coherent structures in the forest canopy: (1) quadrant-hole (Q-H) analysis and (2) wavelet analysis. These two methods are based on different fundamental principles; therefore the comparison of these two methods provides insight into the detection of coherent structures and the resulting contribution to the exchange of energy and mass between forest and canopy. Both methods are described in this section, with additional details provided in the Appendix.

3.1 Quadrant-Hole (Q-H) analysis

Q-H or quadrant analysis is one of many conditional sampling techniques used to study and describe turbulent flows (Antonia, 1981; Lu and Willmarth, 1973). It has been applied to study canopy turbulence in crop (Finnigan, 1979; Shaw et al., 1983; Zhu et al., 2007) and forest ecosystems (Baldochi and Meyers, 1988; Bergstrom and Hogstrom, 1989; Gardiner, 1994; Mortiz, 1989; Thomas and Foken, 2007). Q-H analysis provides information about turbulent structures by separating the fluctuating velocity components (u' and w') into four categories based on sign. Following Shaw et al. (1983), the categories or quadrants are numbered conventionally:

Quadrant 1 (Q1): $u' > 0, w' > 0$ (outward interaction)

Quadrant 2 (Q2): $u' < 0, w' > 0$ (ejection or burst)

Quadrant 3 (Q3): $u' < 0, w' < 0$ (inward interaction)

Quadrant 4 (Q4): $u' > 0, w' < 0$ (sweep)

In the u' versus w' scatter plot in Fig. 2, events are characterized as a “burst” if the $u'w'$ is in Q2, or a “sweep” if $u'w'$ is in quadrant Q4. In most forested canopy studies, the sweep quadrant (Q4) is the largest contributor to momentum transfer within and just above the canopy, and the ejection quadrant (Q2) is the second most important contributor; outward and inward interactions are also components

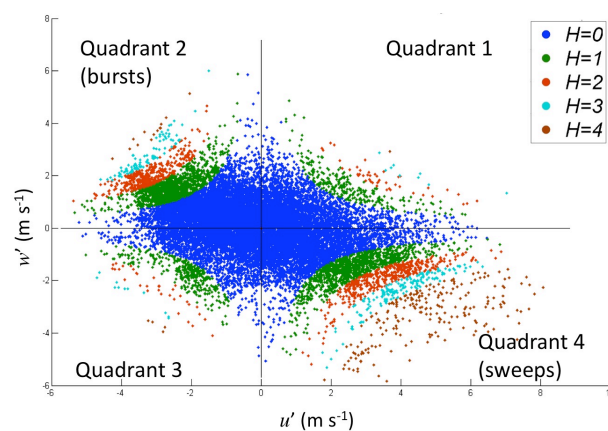


Fig. 2. Sample 30-min analysis (28 July (DOY 209), 12:30–13:00 LT) using the quadrant analysis method for different hole sizes. Each point represents a 10 Hz sonic data point. Note as the hole size increases weak events are excluded, thus for large hole sizes ($H = 4$) only extreme events are considered.

of coherent structures but lead to little exchange within a forested canopy (Finnigan, 2000).

In addition to categorizing the data by quadrant, a threshold parameter (Bogard and Tiederman, 1986) or hole size H (Lu and Willmarth, 1973) is used to separate true burst or sweep events from relatively quiescent motions (Fig. 2). Thus bursts and sweeps are detected when

$$\overline{u'w'} \geq H(u_{\text{rms}}w_{\text{rms}}) \quad (2)$$

where the subscript rms indicates root mean squared velocity. The number and duration of events detected with Q-H analysis are sensitive to the threshold parameter H . Rather than tune H to agree with the wavelet analysis, we used a constant H ($H = 1$) for our analysis as determined by other studies to be a suitable threshold value (Bogard and Tiederman, 1986; Comte-Bellou et al., 1978). Sensitivity of our results to H was evaluated; similar to other studies, we found the number of events decreases quickly with larger hole sizes (see Appendix A) (Baldochi and Meyers, 1988; Bergstrom and Hogstrom, 1989; Mortiz, 1989; Shaw et al., 1983; Zhu et al., 2007). Multiple detections occurring from the same event are separated from independent events using a time frequency parameter (τ). We selected a constant time frequency of $\tau = 0.5 \text{ s}$ based on analyses of several 30-min periods. Additional information on the Q-H method and a sensitivity analysis to H and τ can be found in Appendix A.

3.2 Wavelet analysis

Past studies have successfully implemented the wavelet transform method to identify coherent structures from high-frequency turbulence data (Collineau and Brunet, 1993b; Farge, 1992; Thomas and Foken, 2005). Multiple methods are available for wavelet detection of coherent structures

(Barthlott et al., 2007; Collineau and Brunet, 1993a; Feigenwinter and Vogt, 2005; Lu and Fitzjarrald, 1994; Thomas and Foken, 2005). Here we employ the method of Barthlott et al. (2007), which uses temperature fluctuations to detect ramp structures under stable and unstable conditions. We select this method because the use of temperature ramps provides a physical basis and easy visualization for the selection of coherent structure events.

We apply wavelet analysis to the 10 Hz sonic anemometer temperature records for each 30-min period and use a “Mexican Hat” wavelet, which has been shown to effectively detect coherent structures (e.g., Collineau and Brunet, 1993a; Feigenwinter and Vogt, 2005). For each 30-min time period throughout the field campaign (1152 total periods after pre-processing and filtering), we detect coherent structures according to the following techniques defined in Barthlott et al. (2007). First, we average temperature fluctuations to 1 Hz and remove any temperature trends, and then we calculate the wavelet transform ($W_n(s)$) and global wavelet power spectrum (\overline{W}_s) over a range of scales or periods (s) for each 30-min time interval (see Appendix B for definitions and detailed methodology). We determine the period or time scale that produces the clearly defined local maximum in \overline{W}_s . Then, the wavelet coefficient that corresponds to this maximum period is used to identify coherent structures based on known differences in temperature fluctuations and ramp structures under stable and unstable conditions (Barthlott et al., 2007). Duration of individual events is calculated from the beginning and end times determined above. A sample wavelet analysis that highlights these detection steps is displayed in Fig. B1.

4 Results and discussion

After a brief description of the CABINEX campaign characteristics (Sect. 4.1), the two coherent structure detection methods are examined over the duration of the CABINEX campaign by comparing statistics on the number and duration of events (Sect. 4.2), and the contribution from coherent structures to fluxes of momentum and heat (Sect. 4.3). Because each method uses fundamentally different detection criteria, a side-by-side comparison of the resulting flux contributions can provide CABINEX collaborators with a range of estimates of the contribution of coherent structures to canopy mixing for use in future analyses of chemical and aerosol measurements. Lastly, we compare kinematic heat fluxes between the top and mid-level sonic to determine the degree of coupling between the upper forest canopy and atmosphere (Sect. 4.4).

4.1 CABINEX campaign characteristics

Averaged temperature (\overline{T}), wind speed (\overline{u}) and friction velocity (u_*) derived from the top sonic anemometer data are

Table 1. Statistics of coherent structure detection for the CABINEX campaign, indicating the distribution function median (with standard deviation in parentheses).

	Wavelet	Q-H
Number of structures		
Stable	9.1 (4.9)	300.1 (81.2)
Unstable	5.6 (2.8)	237.5 (49.6)
Duration of structures (s)		
Stable	115.6 (39.6)	1.8 (0.4)
Unstable	90.6 (38.1)	1.3 (0.3)
Momentum flux contribution (%)		
Stable	48.3 (17.3)	43.2 (6.7)
Unstable	39.9 (15.6)	45.3 (7.1)
Heat flux contribution (%)		
Stable	47.5 (16.4)	64.5 (22.0)
Unstable	44.2 (16.0)	60.5 (15.7)
Momentum transport efficiency		
Stable	1.3 (1.3)	2.1 (0.3)
Unstable	1.1 (1.2)	1.9 (0.3)
Heat transport efficiency		
Stable	1.3 (1.4)	3.0 (1.5)
Unstable	1.2 (1.3)	2.5 (1.1)

shown for the entire CABINEX campaign (Fig. 3). Air temperatures measured above the canopy during the campaign are relatively low for the UMBS site compared to average air temperatures in other summers (Bertman et al., 2010) and range between 285–297 K (12–24 °C). Diurnal temperature ranges of up to 10 K occur throughout the campaign, although some periods have warmer nights and reduced temperature ranges (e.g., 22–28 July 2009 or day of year (DOY) 203–209). Wind speeds range from calm to 5 m s⁻¹, with some periods of strong diurnal wind speed variation and others with very little diurnal variation (DOY 203–209). Like temperature, friction velocity provides a good visual trace for the diurnal variations during the campaign, with values ranging from 0–1.2 m s⁻¹. As with temperature and wind speed, relatively low magnitudes of friction velocity (< 0.5 m s⁻¹) occur during the DOY 203–209 time period.

Stability for each 30-min time period is determined by Eq. (1) and a diel plot is shown in Fig. 4. Depending on data availability after filtering (Sect. 2.3), each bar represents 21 to 27 data points (e.g., days). During the campaign, sunrise is at approximately 05:00–05:30 LT and sunset at approximately 20:00–20:30 LT. As expected, stable conditions dominate during the nighttime (22:00–06:00 LT) and characterize 80–90 % of the nighttime 30-min periods. Unstable conditions occur 70–90 % of the time during the daytime (10:00–17:00 LT). All three stability classes occur during transition periods in the morning (06:00–10:00 LT) and

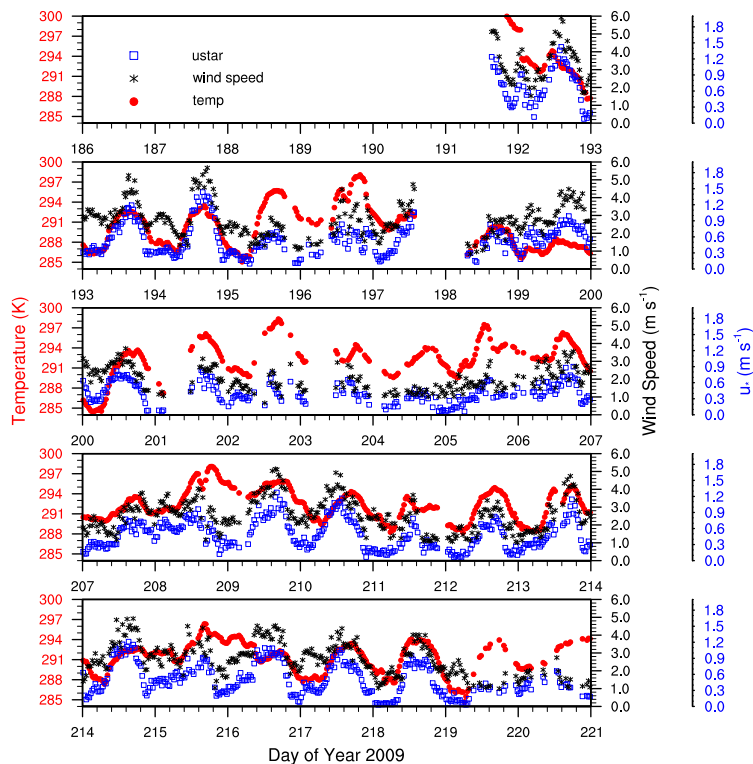


Fig. 3. Time series of filtered meteorological variables from the top sonic anemometer during the 2009 CABINEX campaign (10 July (DOY 191) to 8 August (DOY 220)), including temperature (T , K; red circles), wind speed (\bar{u} , m s^{-1} ; black asterisks), and friction velocity (u_* , m s^{-1} ; blue open squares).

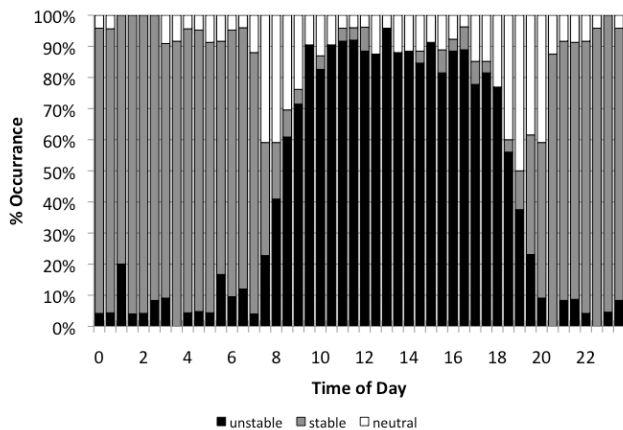


Fig. 4. Diel plot of percent occurrence of stability class (unstable, stable, neutral) for each 30-min period during the CABINEX campaign (10 July–8 August 2009; 27 total days with 1152 total 30-min periods after filtering). Stability classification is based on Obukhov length (Sect. 2.2).

early evening (17:00–22:00 LT) due to substantial changes in the boundary layer dynamics. The relative contribution of neutral conditions (up to 35 % in the early morning and 45 %

in the early evening) increases during these transitional periods compared to daytime and nighttime contributions (typically less than 15 %). Using stability classes only, this suggests very little mixing during the night and transition time periods in and out of daytime. However, the coherent structure analysis described in the remainder of this section provides an alternative view.

4.2 Number and duration of coherent structures

We define the number of coherent structures as the total number of bursts and sweeps within each 30-min time period. The duration of events is defined as the average length (in seconds) of all events for each 30-min period. As discussed in Sect. 3.0, there are fundamental differences between the detection criteria used in the wavelet and Q-H methods. Therefore, a comparative analysis of the statistical results of the two detection methods can help to understand method bias and provide a range of estimates for the coherent structure contribution to turbulent exchange.

A probability distribution function (PDF) and summary statistics of the number of events per 30-min are presented for both analysis methods and for stable and unstable conditions (Fig. 5; Table 1). The number of events determined by Q-H analysis is an order of magnitude greater than the

number of events determined using wavelet analysis (Fig. 5). The wavelet analysis produces distribution functions with a median of 5–9 events depending on stability, while the Q-H analysis produces a median of 237–300 events (Table 1). Both detection methods predict a greater number of events under stable conditions, consistent with the results of Barthlott et al. (2007). The number of events for each method is expected to be different because of underlying detection criteria (Thomas and Foken, 2007). Specifically, the Q-H method detects events when u' and w' signals are above a specified threshold, leading to the potential for false-positive detections and a greater total number of events. Increasing the threshold value H reduces the number of events detected, but does not change the duration of individual events. In contrast, the wavelet method identifies specific events by using temperature fluctuations to detect ramp structures. Because temperature ramps occur over longer time intervals (e.g., tens of seconds), we would expect that the use of ramp structures would lead to a smaller number of longer duration events, potentially biasing detection to miss shorter duration events. Additionally, multiple consecutive events detected by the Q-H method can be considered as a single event by the wavelet analysis.

The above explanation of method discrepancies is supported by an evaluation of average event duration, where differences in the number of coherent structure events are balanced by the predicted total duration of events (Fig. 6). With respect to duration, the wavelet method predicts fewer yet longer events (median times of 91 to 116 s for stable and unstable times, respectively) while the Q-H method predicts shorter durations (median time of 1.3 to 1.8 s for stable and unstable periods, respectively) (Table 1). Again, these differences in the two methodologies are expected because of the varying sensitivity of each detection method and are consistent with other individual method studies. For example, Barthlott et al. (2007) finds average structure duration of approximately 60–65 s under stable conditions and 83–97 s under unstable conditions using the same techniques applied here, whereas Tiederman (1989) found the duration of bursts was between 3–7 s using Q-H analysis for a forested site. For both methods, the average duration of unstable events is approximately 30 % longer than the duration of stable events. This can be physically attributed to an increase in wind shear with increasing stratification, that could lead to shorter, more intense structures under stable conditions (Barthlott et al., 2007).

4.3 Fractional contribution to total flux

The fractional contribution of coherent structures to the total flux is calculated for each 30-min time period (Lu and Fitzjarrald, 1994):

$$F_{\text{coh}} = \frac{\left\{ \sum_{i=1}^n \left(\overline{w'x'_{\text{coh},i}} \times t_{\text{coh},i} \right) \right\}}{\overline{w'x'} \times t} \quad (3)$$

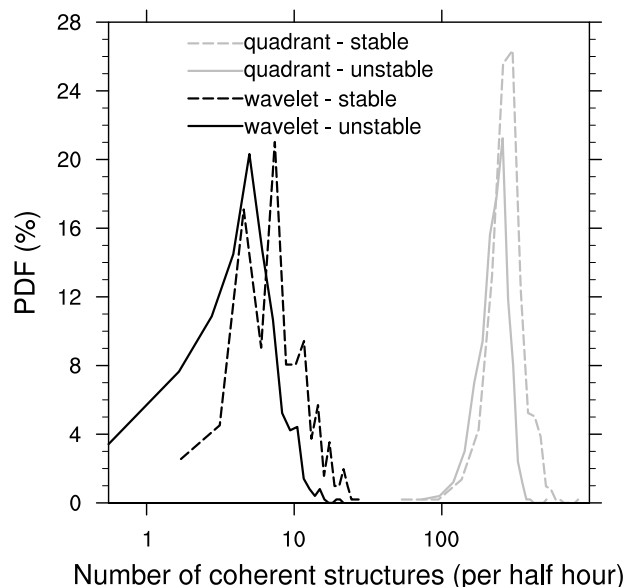


Fig. 5. Probability distribution function of the number of coherent structures per 30-min for the Q-H (gray) and wavelet methods (black) under stable (dashed lines) and unstable (solid lines) conditions.

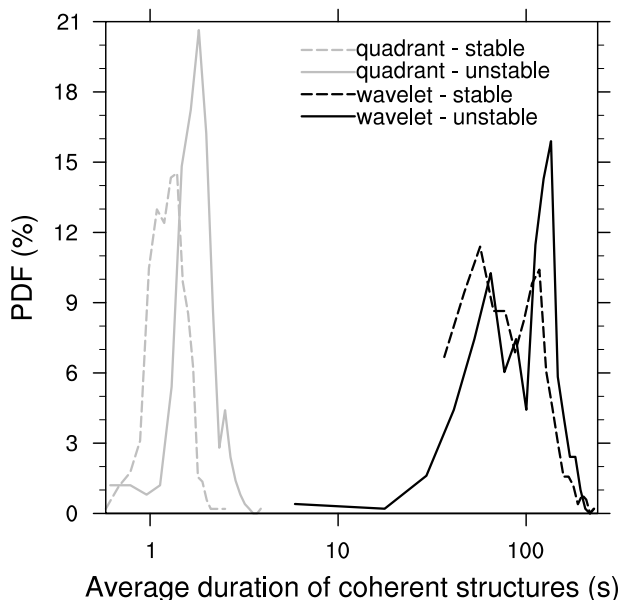


Fig. 6. Probability distribution function of the average duration of coherent structures (in seconds) for the Q-H (gray) and wavelet (black) methods under stable (dashed lines) and unstable (solid lines) conditions.

where $\overline{w'x'}$ is the vertical kinematic flux of variable x over the full 30-min time period (t), $\overline{w'x'_{\text{coh}}}$ is the vertical kinematic flux of variable x during the coherent structure, t_{coh} is

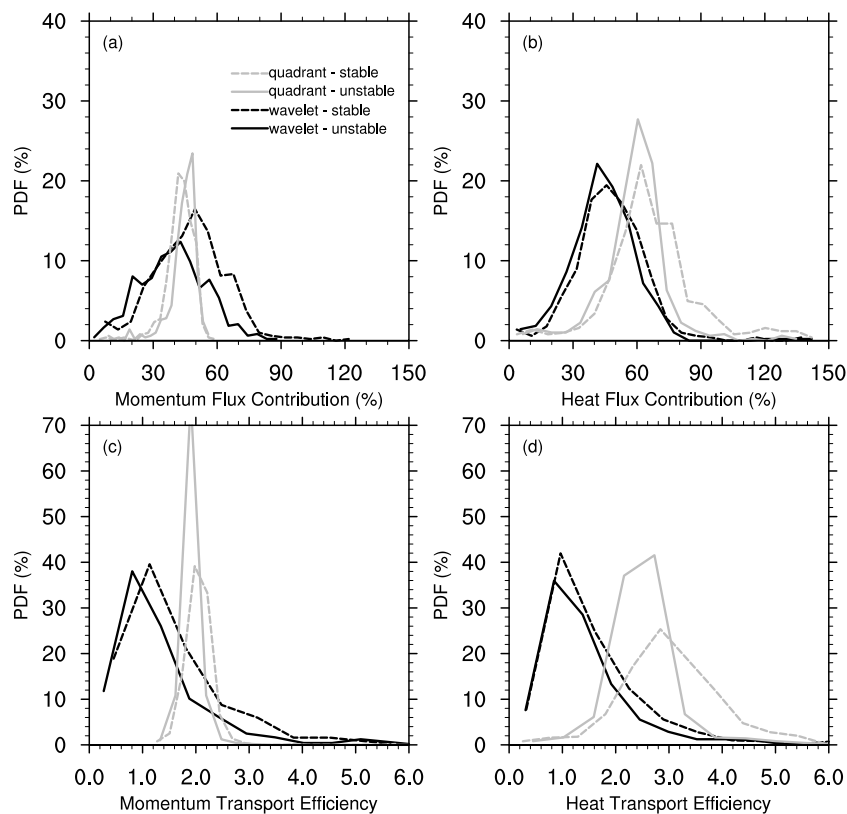


Fig. 7. Probability distribution function of (a) percent contribution to kinematic momentum flux, (b) percent contribution to kinematic heat flux, (c) momentum transport efficiency, and (d) heat transport efficiency for the Q-H (gray lines) and wavelet (black lines) methods under stable (dashed) and unstable (solid) conditions.

the duration of the coherent structure, and n is the number of events during the 30-min time period. For each method (wavelet and Q-H), we calculate the fractional contribution of the coherent structures to the kinematic momentum flux (F_m , $\overline{u'w'}$) and kinematic heat flux (F_h , $\overline{w'T'}$). We also assess the relative efficiency (E) of these contributions by normalizing F_{coh} to the percentage of time they occupy within each half-hour period (TC) (Barthlott et al., 2007):

$$TC = \frac{\sum_{i=1}^n t_{\text{coh},i}}{t} \quad (4)$$

$$E = \frac{F_{\text{coh}}}{TC} \quad (5)$$

Values of E greater than one indicate that the structures are more efficient at transporting heat or momentum, with increasing E values indicating greater efficiency.

The wavelet and Q-H methods yield similar fractional flux contributions of 40–48 % to total F_m from coherent structures (Fig. 7a and Table 1). F_m contributions are slightly higher under stable conditions in the wavelet analysis, and slightly lower under stable conditions in the Q-H analysis.

As noted above, this is likely due to an increase in the generation of structures with increasing stratification. In general, the Q-H analysis shows a narrower distribution than the wavelet analysis similar to the number and duration of events (Figs. 5 and 6), yet the resulting median values are similar. The efficiency of these structures for momentum transport (Fig. 7c) varies between the two methods, with greater efficiency by the Q-H method (median value of approximately 2). The median efficiency for the wavelet method is slightly greater than one (1.1 for unstable conditions and 1.3 for stable conditions), yet some structures can be up to four times as efficient as averaged fluxes as evidenced by the large standard deviation. For both methods, efficiencies are greater under stable than unstable conditions, which may be indicative of the increased importance of these structures under stratified conditions.

For F_h , the wavelet method shows a similar F_{coh} as for F_m , with a median contribution of approximately 40–50 % (and with a similar standard deviation) and slightly greater contributions under stable conditions. The Q-H analysis indicates a slightly greater contribution of coherent structures to the kinematic heat flux, with median values of approximately 60–65 %. Standard deviation values and a slight

increase in contributions under stable conditions are similar to the wavelet analysis. Efficiencies of kinematic heat flux are similar to the momentum transport efficiencies for the wavelet method, but are greater than momentum fluxes for the Q-H method. Both methods indicate that heat transport efficiencies are greater under stable conditions. This result is consistent with Barthlott et al. (2007), who found that the coherent structures were slightly more efficient in their transport of heat than momentum. The relative contribution of coherent structures to heat or momentum transport is still unresolved in the literature; for example, some studies show that the contributions are roughly equal (Gao et al., 1989; Lu and Fitzjarrald, 1994), others indicate that momentum fluxes are higher (Bergstrom and Hogstrom, 1989), and others suggest that the heat flux contribution is greater (Barthlott et al., 2007; Collineau and Brunet, 1993b; Feigenwinter and Vogt, 2005). Reasons why coherent structures may differ in their transport of heat and momentum are uncertain, yet have implications for atmospheric chemistry. F_h and the eddy diffusivity for heat (K_h) are generally used as a proxy for other scalar transport, and we could expect that coherent structures might contribute slightly more to the exchange of gases and aerosols. Despite similar magnitude of flux contributions, the two methods presented here show conflicting results on the contributions to kinematic heat versus momentum flux. F_m contributions are similar for both methods and F_h contributions show an increase with Q-H analysis over wavelet analysis. This is consistent with the transport efficiencies, where momentum and heat efficiencies are similar in the wavelet analysis and greater for heat than momentum in the Q-H analysis, suggesting that these differences may be method dependent.

Overall, the flux contributions using each method are similar despite the differences in the methods implemented to identify and classify coherent structures. That is, the Q-H analysis method detects more frequent, shorter and more efficient events while the wavelet method detects less frequent, longer events that are only slightly more efficient at transporting fluxes than non-events. Resulting flux contributions from each method are likely similar because coherent-structure contributions are dominated by very large events that are likely detected by both methods. Finnigan (1979) and Shaw et al. (1983) found that half of the total contribution to momentum flux from sweeps comes from events when $u'w' > 10|\overline{u'w'}|$; i.e., events so large that they are likely to be detected by either method. Thomas and Foken (2007) compared the wavelet analysis and Q-H analysis and found that they can produce fundamentally different results, and favored wavelet analysis for identifying specific event times and locations. However, our findings at the CABINEX site suggest that the flux contribution estimates are not sensitive to the detection method yet the Q-H method estimates more efficient coherent structures than the wavelet method.

4.4 Canopy-atmosphere coupling strength

In CABINEX, measurements from two anemometers are available to determine the degree of upper canopy-atmosphere coupling, as in (Thomas and Foken, 2007). We compare kinematic heat flux above the canopy ($H_{\text{tot},1.5\text{h}}$) and the kinematic heat flux measured within the upper canopy ($H_{\text{tot},0.92\text{h}}$). Positive ratios suggest that the fluxes are moving in the same direction and indicate coupling between the canopy and atmosphere. Following Thomas and Foken (2007), we use the relationship between $H_{\text{tot},1.5\text{h}}$ and $H_{\text{tot},0.92\text{h}}$ to define a “strength” threshold for canopy-atmosphere coupling. A regression between these two fluxes above a minimum value of 0.2 ($H_{\text{tot}} \geq 0.2 \text{ K m s}^{-1}$; signifying a substantial value) yields a slope of 0.68 (Fig. 8), and the inverse of the high flux slope ($1/0.68 = 1.47$) determines the threshold of coupling between canopy and atmosphere. If the ratio of $H_{\text{tot},1.5\text{h}}/H_{\text{tot},0.92\text{h}}$ is greater than zero and below the threshold, then the canopy and atmosphere are considered to be “strongly coupled,” as the magnitude of fluxes are relatively similar. If the ratio exceeds the threshold value and is positive, then the flux of heat is in the same direction yet the flux above canopy is much stronger than the in-canopy flux. This suggests a “weakly coupled” canopy and atmosphere. Negative ratios indicate opposing flux direction and suggest the canopy is uncoupled from the atmosphere.

The canopy and atmosphere tend to be either strongly or weakly coupled over the duration of the CABINEX campaign (Fig. 9). Between 10:00–18:00 LT, the canopy and atmosphere are almost always coupled, with strongly coupled conditions occurring 56 % of the time and weakly coupled conditions occurring 42 % of the time. During the night (22:00–04:00 LT), $H_{\text{tot},1.5\text{h}}/H_{\text{tot},0.92\text{h}}$ suggests that the canopy is still coupled to the atmosphere with strong and weak conditions occurring 68 % and 27 % of the time. There are several instances of uncoupled conditions throughout the diurnal cycle, predominantly in the early morning (04:00–09:00 LT). The greatest instance of uncoupled conditions occurs at 08:00 LT, which occurs 30 % of the time over the full campaign period. This analysis of the diurnal cycle suggests that coupling occurs between the canopy and atmosphere most of the time, with early morning hours leading to the greatest number of uncoupled conditions.

Figure 10 identifies the coupling conditions over the full time period of the CABINEX campaign. This time series highlights the dominance of strong and weakly coupled conditions identified in Fig. 9, and also identifies specific days when uncoupled conditions occur in the early morning. This figure can provide guidance for other CABINEX participants on the vertical mixing in the upper portion of the canopy and identify time periods of strong mixing.

5 Conclusions

We present an analysis of the contribution of coherent structures to vertical fluxes of heat and momentum during the CABINEX campaign 10 July to 8 August 2009 at the University of Michigan Biological Station. Two techniques, the quadrant-hole analysis and the wavelet analysis, were used to identify the contribution of coherent structures to fluxes of momentum and heat between the canopy and the atmosphere. While the two methods represent fundamentally disparate ideas about how coherent structures can be detected, they demonstrate that the contribution of these structures to turbulent canopy exchange is 40–48 % of the kinematic momentum flux and 44–65 % of the kinematic heat flux. We also identify time periods of uncoupled, weakly coupled, or strongly coupled canopy-atmosphere relationships during the campaign, which can highlight specific time periods of well-mixed canopy-atmosphere air. The upper canopy and atmosphere are coupled the majority of the campaign period, however, uncoupled canopy-atmosphere events occur in the early morning (04:00–08:00 LT) approximately 30 % of the time.

There are an increasing number of field campaigns conducting atmospheric chemistry gradient measurements at multiple levels throughout the forest canopy, often without support from micrometeorologists. While prior micrometeorological studies have performed coherent structure analysis for contributions to fluxes and canopy-atmosphere coupling analysis (e.g., Thomas and Foken, 2007), there has been little interaction with the atmospheric chemistry community. The results presented here provide an example of how these techniques can be applied to explain mixing within the forest canopy, a key element for understanding atmospheric chemical gradients within and above forest canopies. The implications of this increased vertical mixing on atmospheric chemistry are explored in a separate paper in this Special Issue (Bryan et al., 2011), which will incorporate the impacts of vertical mixing on modeled gradients of atmospheric constituents.

Current atmospheric chemistry models do not include any method to assess coherent structures, and typically rely on traditional K -theory to explain mixing within a forest canopy. One exception is the use of large-eddy simulation (LES) models, which capture some of these types of canopy-atmosphere exchange (Edburg, 2009; Patton et al., 2001; Yue et al., 2007), yet these models are rarely coupled with full chemical modeling due to computational constraints. Our results show that the coherent structures will likely contribute significantly to the canopy-atmosphere mixing during most periods. Somewhat counter intuitive to traditional stability analysis, coherent structures continue to play a role in transport at night which leads to coupled canopy-atmosphere conditions, a process missed by most atmospheric chemistry models.

We suggest future atmospheric chemistry field campaigns include multiple levels of meteorological measurements

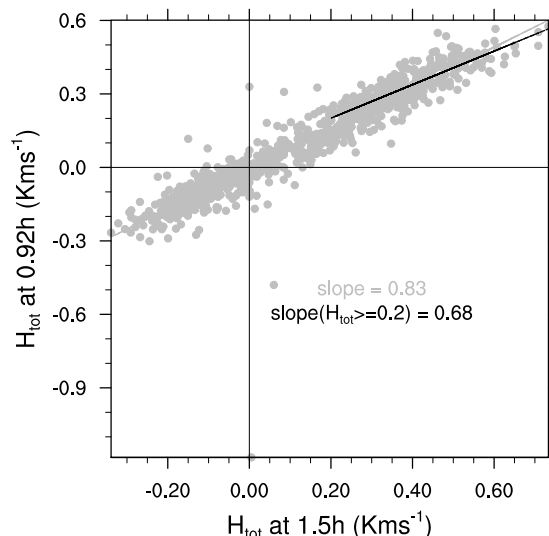


Fig. 8. Scatter plot of the coherent structure contribution to kinematic heat flux (H_{tot}) between the two heights (top; 1.5 h and mid; 0.92 h). The black line represents the slope of total heat flux greater than 0.2 K m s^{-1} .

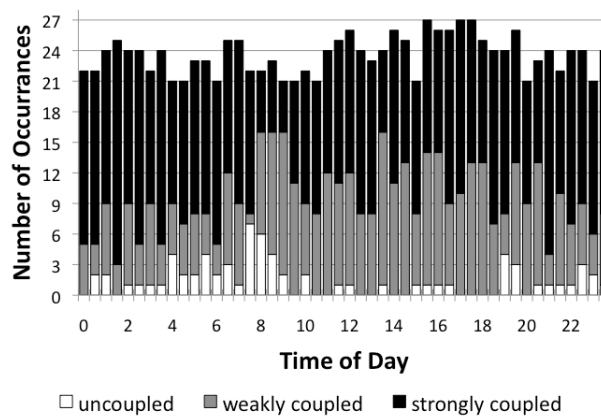


Fig. 9. Number of occurrences of strongly coupled, weakly coupled, or uncoupled atmosphere-canopy relationships over the time period of the campaign (time period as in Fig. 4).

within and above canopies as well as numerical modeling. The CABINEX campaign utilized data from two sonic anemometers, though clearly more information about the sub-canopy and in-canopy coupling is needed (Thomas and Foken, 2007). We note here that this analysis uses sonic data from the upper portion of the canopy, and therefore does not reflect the full coupling between the understory and the atmosphere. Further instrumentation in future studies would be required to assess the below canopy coupling. These experimental designs are needed to quantify the role of in-canopy chemical processing and exchange and separate sub-canopy processes from the upper canopy.

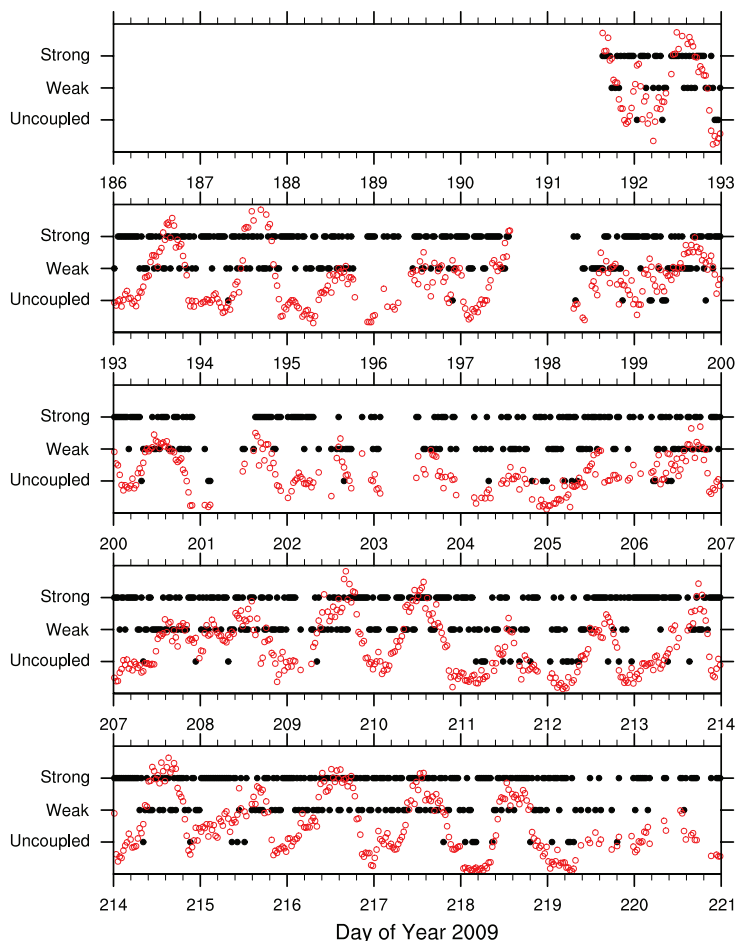


Fig. 10. Time series of coupling over the duration of the campaign (black closed circles). Friction velocity (red open circles) is shown for reference.

Appendix A

Quadrant hole (Q-H) method and sensitivity study

The Q-H analysis detects an event based on a threshold parameter, H , which is used to separate background turbulence from coherent structure events (Fig. 2). Ideally, the number of events detected would be constant for a range of threshold parameters as in (Wells, 1998); however, this is not true for turbulence above forest canopies (Baldocchi and Meyers, 1988). As in Baldocchi and Meyers (1988), we found that the number of events and event duration decreases as H increases (Fig. A1) and thus the contribution to momentum and heat flux decreases. Based on these results, we used a constant hole-size ($H = 1$) for all analyses to eliminate background turbulence while maintaining a reasonable number of event detections.

After events are detected with the Q-H method, multiple detections of the same event are grouped using a time frequency parameter τ (τ), defined as the maximum time

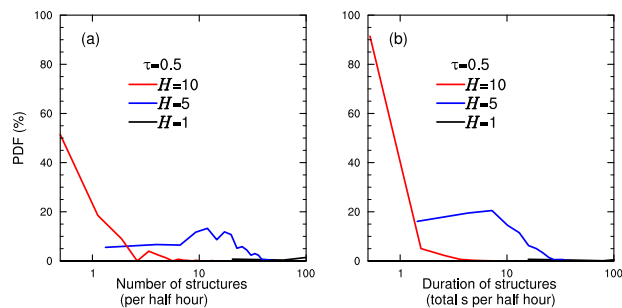


Fig. A1. Probability distribution function of (a) the kinematic momentum flux contribution and (b) kinematic heat flux contribution of coherent structures for the Q-H method for a constant time frequency parameter ($\tau = 0.5$ s) and a range of hole-sizes ($H = 1-10$).

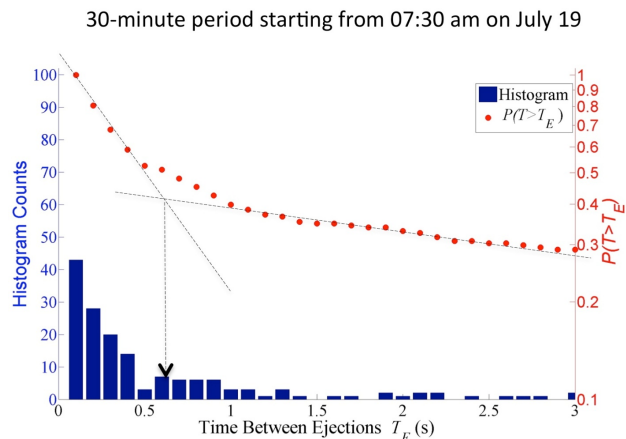


Fig. A2. Sample histogram (left axis) and cumulative probability distribution (right axis) of time between ejections (T_E (s)) for a single 30-min period (07:30 LT on 19 July 2009). τ , the maximum time between ejections of the same burst event, can be estimated by the minimum in the histogram or the intersections of the two asymptotic lines in the plot of the cumulative probability distribution on a logarithmic scale against T_E (Luchik and Tiederman, 1987; Tiederman, 1989).

between ejections from the same burst. τ is obtained by plotting the histogram or cumulative probability function of the time between events and visually detecting two distinctly different statistical regions: a region of multiple ejections within a single burst, and a region of independent detections from different bursts (Luchik and Tiederman, 1987; Tiederman, 1989) (Fig. A2). We conducted this analysis for several half hour periods spanning multiple days during CABINEX, and found a range of τ between 0.3 to 1.5 s. We then conducted a sensitivity study on a range of τ (Fig. A3) and found the variation in both number of structures and duration of structures using the range of τ values is low. Therefore, we used a constant $\tau = 0.5$ s for all periods in the CABINEX analysis.

Appendix B

Wavelet analysis and sensitivity tests

Wavelet analysis is a method frequently employed to detect coherent structures (Collineau and Brunet, 1993b; Gao et al., 1989; Kumar and Foufoula-Georgiou, 1994; Thomas and Foken, 2007). Application of wavelet analysis to canopy-scale turbulence can depict variations of power within a time series, where sharp changes in power at specific points in the time series represent the presence of a coherent structure. This provides additional information as compared to Fourier transforms, which analyze variations of power yet lose the time component of the analysis.

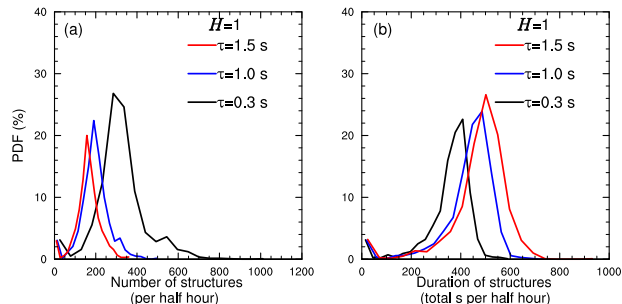


Fig. A3. Probability distribution function of (a) the number of coherent structures and (b) the average duration of coherent structures (seconds) for the Q-H method for a constant hole-size ($H = 1$) and a range of time frequency parameters ($\tau = 0.3–1.5$ s).

The wavelet method defines a continuous wavelet transform $W_n(s)$ for a variable $x(t)$ (e.g., temperature) using a wavelet $\psi(t)$ as an integration kernel (Kumar and Foufoula-Georgiou, 1994):

$$W_n(s) = \frac{1}{s} \int_{-\infty}^{\infty} x(t) \Psi\left(\frac{t-n}{s}\right) \quad (\text{B1})$$

where n is a position translation, s is a scale dilation, and the wavelet $\psi(t)$ is a real or complex-valued function with zero mean (Barthlott et al., 2007). The scale dilation, s , allows the broadening or narrowing of $\psi(t)$, and n shifts the time of the $\psi(t)$ origin. By changing s over a time series, the amplitude and scale of turbulence can be visualized (Torrance and Campo, 1998). The wavelet variance (also called the global wavelet spectrum; \bar{W}_s) yields the integrated energy content at a specific s , providing a representative scale of the coherent structures and corresponding to the mean structure duration.

As noted in Sect. 3.2 we employ the Barthlott et al. (2007) method of wavelet analysis and coherent structure detection. This specific detection technique uses temperature fluctuations to detect ramp structures under stable and unstable conditions. We employ the “Mexican Hat” wavelet to detect ramps (Collineau and Brunet, 1993a; Feigenwinter and Vogt, 2005), because the second derivative of the signal creates a change in sign at discontinuities in a similar manner as temperature ramps (Barthlott et al., 2007). For each 30-min time period throughout the field campaign, we detect coherent structures according to the following steps:

1. Average temperature perturbations to 1 Hz and detrend each 30-min time period (Fig. B1a);
2. Calculate the wavelet function (Fig. B1b) and wavelet power spectrum (Fig. B1c) for each 30-min time period;
3. Determine the period that produces the greatest power, by finding a clearly defined local maximum in the global

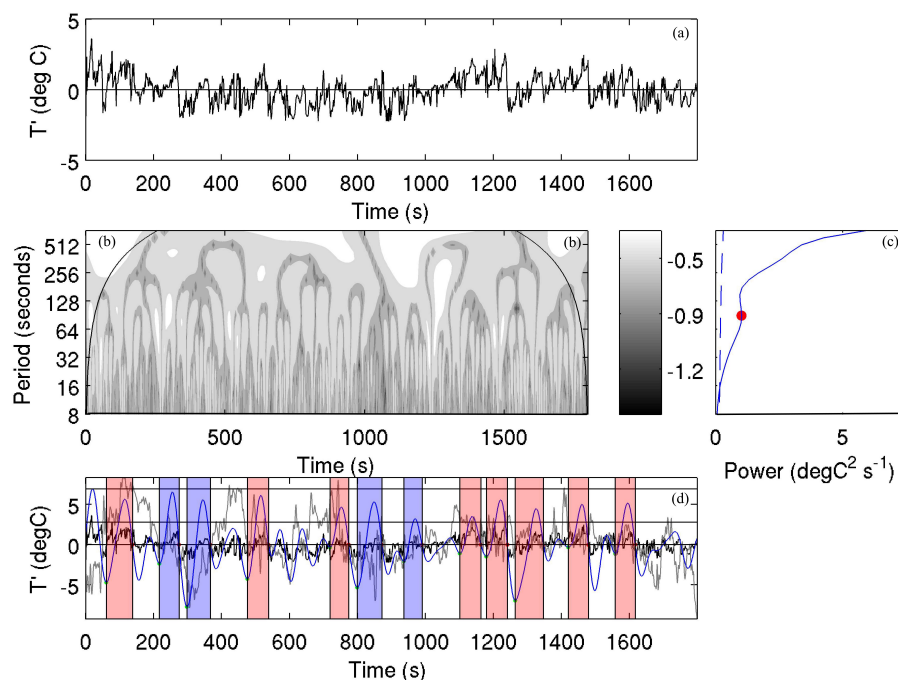


Fig. B1. Sample wavelet analysis for a single 30-min period (14:30 LT on 28 July 2009) based on the Barthlott et al. (2007) detection method. (a) Temperature perturbation from the mean (K), (b) Wavelet period versus time, (c) Global wavelet spectrum, with the peak power (red dot), which selects the power for the wavelet spectrum for this half hour, and (d) plot of temperature perturbation (T' ; black line), vertical wind perturbation (w' ; gray line), wavelet (blue line), and detected burst periods (w' positive; red shaded regions) and sweep periods (w' negative; blue shaded regions).

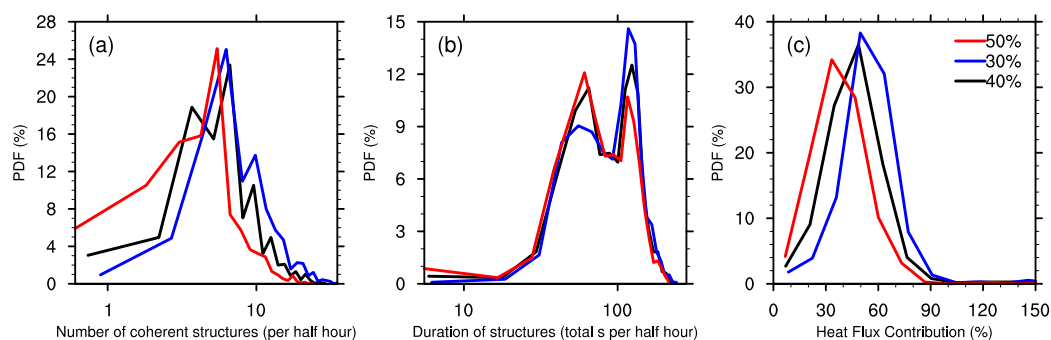


Fig. B2. Sensitivity analysis of wavelet technique to the wavelet power spectrum threshold criteria of 40 % (black; used in the paper analysis), 30 % (blue) and 50 % (red) for the (a) number of coherent structures, (b) duration of structures, and (c) percent contribution to kinematic heat flux.

wavelet spectrum (Barthlott et al., 2007; red dot in Fig. B1c).

- Identify the coherent structures based on known differences in temperature fluctuations and ramp structures under stable and unstable conditions (Barthlott et al., 2007). Stable-condition ramp structures have a sharp increase in temperature followed by a slow decrease (black line; Fig. B1d), and can be detected by a zero-

crossing of the global wavelet spectrum, followed by local maximum, followed by a local minimum in the wave function (blue line; Fig. B1d). Unstable-condition ramp structures have a slow increase in temperature followed by a sharp drop (Barthlott et al., 2007), and unstable and neutral time periods are detected by a series of local minimum in the global wavelet power spectrum, followed by local maximum, followed by a zero-crossing of the wave function. For a local maximum to

be considered a defined peak, it has to reach a positive value at or greater than 40 % of the maximum value for that wave function in the 30-min time period, thereby eliminating small peaks and fluctuations (Barthlott et al., 2007; Collineau and Brunet, 1993a).

- Identify the direction of the coherent structure based on the average w' value within the specific structure (Fig. B1d; grey line) (e.g., a w' greater than zero indicates a burst, while a w' less than zero indicates a sweep). For further ease of visual analysis of these structures, coherent structure time intervals designated as bursts are shaded red and sweeps are shaded blue.

Over the full campaign, these analysis steps are repeated for each 30-min time period to identify the number of coherent structures and their duration. Statistics for the full campaign are presented in Figs. 5 and 6.

The wavelet analysis results are insensitive to the selection of s and time interval (t), but do exhibit slight sensitivity to the 40 % cutoff criteria (Fig. B2). Decreasing (increasing) the criteria by ± 10 % decreased (increased) the number of structures detected per half hour, leading to a decrease (increase) of contribution of coherent structures to the kinematic heat flux by shifting the median value by approximately 5 %. While this can make slight differences in the contribution numbers, the conclusion that coherent structures contribute to the kinematic heat flux remains robust.

Acknowledgements. We gratefully acknowledge the entire CABINEX team, led by S. Bertman, M.A. Carroll, P. Shepson and P. Stevens for their logistical support and assistance. We also thank C. S. Vogel of UMBS for providing precipitation data from the AmeriFlux tower. Wavelet analysis was possible due to software provided by C. Torrence and G. Compo (available at <http://atoc.colorado.edu/research/wavelets>). Funding for this work was provided by the National Science Foundation ATM-0904128 to A. L. Steiner at the University of Michigan (UM) and ATM-0904214 to S. N. Pressley and S. H. Chung at Washington State University (WSU). Additional support was also provided through the Research Experience for Undergraduates (REU) program at UM to support A. Botros (ATM-0552353) and WSU to support E. Jones (ATM-0754990), and through the Biosphere Atmosphere Research and Training NSF IGERT program to support S. L. Edburg.

Edited by: J. Fuentes

References

- Antonia, R. A.: Conditional sampling in turbulence measurements, *Annu. Rev. Fluid Mech.*, 13, 131–156, 1981.
- Baldocchi, D. D. and Meyers, T. P.: Turbulence structure in a deciduous forest, *Bound.-Lay. Meteorol.*, 43, 345–364, 1988.
- Baldocchi, D. D., Falge, E., Gu, L., Olson, R., Hollinger, D., Running, S., Anthoni, P., Bernhofer, C., Davis, K., Evans, R., Fuentes, J., Goldstein, A., Katul, G., Law, B., Lee, X., Malhi, Y., Meyers, T., Munger, W., Oechel, W., Paw U., K. T., Pilegaard, K., Schmid, H. P., Valentini, R., Verma, S., Vesala, T., Wilson, K., and Wofsy, S.: FLUXNET: A New Tool to Study the Temporal and Spatial Variability of Ecosystem-Scale Carbon Dioxide, Water Vapor and Energy Flux Densities, *B. Am. Meteorol. Soc.*, 82, 2415–2435, 2001.
- Barthlott, C., Drobinski, P., Fesquet, C., Dubos, T., and Pietras, C.: Long-term study of coherent structures in the atmospheric surface layer, *Bound.-Lay. Meteorol.*, 125, 1–24, 10.1007/s10546-007-9190-9, 2007.
- Bergstrom, H. and Hogstrom, U.: Turbulent exchange above a forest, II: Organized structures, *Bound.-Lay. Meteorol.*, 49, 231–263, 1989.
- Bertman, S. B., Carroll, M. A., Shepson, P. B., and Stevens, P. S.: Overview of CABINEX/PROPHET 2009, Fall Meeting, American Geophysical Union, San Francisco, CA, Abstract A53C-0234, 2010.
- Bogard, D. G. and Tiederman, W. G.: Burst detection with single-point velocity measurements, *J. Fluid. Mech.*, 162, 389–413, 1986.
- Brunet, Y. and Irvine, M. R.: The control of coherent eddies in vegetation canopies: Streamwise structure spacing, canopy shear scale and atmospheric stability, *Bound.-Lay. Meteorol.*, 94, 139–163, 2000.
- Bryan, A. M., Forkel, R., Bertman, S. B., Carroll, M. A., Dusanter, S., Edwards, G. D., Griffith, S., Guenther, A. B., Hansen, R. F., Jobson, T., Keutsch, F. N., Lefer, B. L., Pressley, S. N., Shepson, P. B., Stevens, P. S., and Steiner, A. L.: In-canopy gas-phase chemistry during the 2009 CABINEX field campaign: Sensitivity to isoprene chemistry and vertical mixing, in preparation, 2011.
- Carroll, M. A., Shepson, P. B., and Bertman, S. B.: Overview of the Program for Research on Oxidants: Photochemistry, Emissions and Transport (PROPHET) Summer 1998 measurements intensive, *J. Geophys. Res.-Atmos.*, 106, 24275–24288, 2001.
- Collineau, S. and Brunet, Y.: Detection of turbulent coherent motions in a forest canopy, 1. Wavelet analysis, *Bound.-Lay. Meteorol.*, 65, 357–379, 1993a.
- Collineau, S. and Brunet, Y.: Detection of turbulent coherent motions in a forest canopy, Part 2: Time-scales and conditional averages, *Bound.-Lay. Meteorol.*, 66, 49–73, 1993b.
- Comte-Bellou, G., Sabot, J., and Saleh, I.: Detection of intermittent events maintaining Reynolds stress, *Proc. Dynamic Flow Conf. – Dynamic Measurements in Unsteady Flows*, 1978.
- Dlugi, R., Berger, M., Zelger, M., Hofzumahaus, A., Siese, M., Holland, F., Wisthaler, A., Grabmer, W., Hansel, A., Koppmann, R., Kramm, G., Möllmann-Coers, M., and Knaps, A.: Turbulent exchange and segregation of HOx radicals and volatile organic compounds above a deciduous forest, *Atmos. Chem. Phys.*, 10, 6215–6235, doi:10.5194/acp-10-6215-2010, 2010.
- Edburg, S.: A numerical study of turbulence, dispersion and chemistry within and above forest canopies, Ph.D., College of Engineering and Architecture, Washington State University, Pullman, 2009.
- Farge, M.: Wavelet transforms and their applications to turbulence, *Annual Reviews of Fluid Mechanics*, 24, 395–457, 1992.

- Feigenwinter, C. and Vogt, R.: Detection and analysis of coherent structures in urban turbulence, *Theor. Appl. Climatol.*, 81, 219–230, 2005.
- Finnigan, J.: Turbulence in plant canopies, *Annu. Rev. Fluid Mech.*, 32, 519–571, 2000.
- Finnigan, J. J.: Turbulence in waving wheat: II. Structure of momentum transfer, *Bound.-Lay. Meteorol.*, 16, 213–236, 1979.
- Finnigan, J. J., Shaw, R. H., and Patton, E. G.: Turbulence structure above a vegetation canopy, *J. Fluid Mech.*, 637, 387–424, 2009.
- Foken, T.: *Micrometeorology*, Springer-Verlag, Berlin, 306 pp., 2008.
- Fuentes, J. D., Wang, D., Bowling, D. R., Potosnak, M., Monson, R. K., Goliff, W. S., and Stockwell, W. R.: Biogenic hydrocarbon chemistry within and above a mixed deciduous forest, *J. Atmos. Chem.*, 56, 165–185, 2007.
- Gao, W., Shaw, R. H., and Paw U, K. T.: Observation of organized structure in turbulent flow within and above a forest canopy, *Bound.-Lay. Meteorol.*, 47, 349–377, 1989.
- Gardiner, B.: Wind and wind forests in a plantation spruce forest, *Bound.-Lay. Meteorol.*, 67, 161–186, 1994.
- Harman, I. N. and Finnigan, J. J.: Scalar concentration profiles in the canopy and roughness sublayer, *Bound.-Lay. Meteorol.*, 129, 323–351, 2008.
- Holzinger, R., Lee, A., Paw, K. T., and Goldstein, U. A. H.: Observations of oxidation products above a forest imply biogenic emissions of very reactive compounds, *Atmos. Chem. Phys.*, 5, 67–75, doi:10.5194/acp-5-67-2005, 2005.
- Katul, G. G., Mahrt, L., Poggi, D., and Sanz, C.: One- and two equation models for canopy turbulence, *Bound.-Lay. Meteorol.*, 113, 81–109, 2004.
- Kumar, P. and Foufoula-Georgiou, F.: Wavelet analysis in geophysics: An introduction, in: *Wavelets in Geophysics*, edited by: Foufoula-Georgiou, E. and Kumar, P., Academic Press, San Diego, 372 pp., 1994.
- Law, B. E., Falge, E., Gu, L., Baldocchi, D. D., Bakwin, P., Berbigier, P., Davis, K., Dolman, A. J., Falk, M., Fuentes, J. D., Goldstein, A., Granier, A., Grelle, A., Hollinger, D., Janssens, I. A., Jarvis, P., Jensen, N. O., Katul, G., Mahli, Y., Matteucci, G., Meyers, T., Monson, R., Munger, W., Oechel, W., Olson, R., Pilegaard, K., Paw, K. T., Thorgeirsson, H., Valentini, R., Verma, S., Vesala, T., Wilson, K., and Wofsy, S.: Environmental controls over carbon dioxide and water vapor exchange of terrestrial vegetation, *Agric. For. Meteorol.*, 113, 97–120, 2002.
- Lu, C.-H. and Fitzjarrald, D. R.: Seasonal and diurnal variations of coherent structures over a deciduous forest, *Bound.-Lay. Meteorol.*, 69, 43–69, 1994.
- Lu, S. S. and Willmarth, W. W.: Measurements of the structure of the Reynolds stress in a turbulent boundary layer, *J. Fluid Mech.*, 60, 481–511, 1973.
- Luchik, T. S. and Tiederman, W. G.: Timescale and structure of ejections and bursts in turbulent channel flows, *J. Fluid Mech.*, 174, 529–552, 10.1017/S0022112087000235, 1987.
- Moeng, C.-H.: A large-eddy simulation model for the study of planetary boundary-layer turbulence, *J. Atmos. Sci.*, 45, 3573–3587, 1984.
- Mortiz, E.: Heat and momentum transport in an oak forest canopy, *Bound.-Lay. Meteorol.*, 49, 317–329, 1989.
- Nietz, J. G.: Soil respiration during partial canopy senescence in a northern mixed deciduous forest, M.S., *Ecology and Organismal Biology*, The Ohio State University, 110 pp., 2010.
- Oncley, S. P., Foken, T., Vogt, R., Kohsiek, W., DeBruin, H. A. R., Bernhofer, C., Christen, A., van Gorsel, E., Grantz, D., Feigenwinter, C., Lehner, I., Liebenthal, C., Liu, H., Mauder, M., Pitacco, A., Ribeiro, L., and Weidinger, T.: The Energy Balance Experiment EBEX-2000. Part I: Overview and energy balance, *Bound.-Lay. Meteorol.*, 123, 1–28, doi:10.1007/s10546-007-9161-1, 2007.
- Patton, E. G., Davis, K., Barth, M. C., and Sullivan, P. P.: Decaying scalars emitted by a forest canopy: A numerical study, *Bound.-Lay. Meteorol.*, 100, 91–129, 2001.
- Raupach, M. R.: Conditional statistics of Reynolds's stress in rough wall and smooth wall turbulent boundary layers, *J. Fluid Mech.*, 108, 363–382, 1981.
- Raupach, M. R. and Thom, A. S.: Turbulence in and above plant canopies, *Annu. Rev. Fluid Mech.*, 13, 97–129, 1981.
- Raupach, M. R., Finnigan, J. J., and Brunet, Y.: Coherent eddies and turbulence in vegetation canopies: The mixing-layer analogy, *Bound.-Lay. Meteorol.*, 78, 351–382, 1996.
- Rizzo, L. V., Artaxo, P., Karl, T., Guenther, A. B., and Greenberg, J.: Aerosol properties, in-canopy gradients, turbulent fluxes and VOC concentrations at a pristine forest site in Amazonia, *Atmos. Environ.*, 44, 503–511, 2010.
- Shaw, R. H., Tavangar, J., and Ward, D. P.: Structure of Reynolds stress in a canopy layer, *J. Clim. Appl. Meteorol.*, 22, 1922–1931, 1983.
- Sörgel, M., Trebs, I., Serafimovich, A., Moravek, A., Held, A., and Zetzsch, C.: Simultaneous HONO measurements in and above a forest canopy: influence of turbulent exchange on mixing ratio differences, *Atmos. Chem. Phys.*, 11, 841–855, doi:10.5194/acp-11-841-2011, 2011.
- Su, H.-B., Schmid, H. P., Vogel, C. S., and Curtis, P. S.: Effects of canopy morphology and thermal stability on mean flow and turbulence statistics observed inside a mixed hardwood forest, *Agr. For. Meteorol.*, 148, 862–882, 2008.
- Thomas, C. and Foken, T.: Detection of long-term coherent exchange over spruce forest using wavelet analysis, *Theor. Appl. Climatol.*, 80, 91–104, doi:10.1007/s00704-004-0093-0, 2005.
- Thomas, C. and Foken, T.: Flux contribution of coherent structures and its implications for the exchange of energy and matter in a tall spruce canopy, *Bound.-Lay. Meteorol.*, 123, 317–337, 10.1007/s10546-006-9144-7, 2007.
- Tiederman, W. G.: Eulerian detection of turbulent bursts, *Near Wall Turbulence*, Proc. Z. Zoriac Memorial conference, 874–447, 1989.
- Torrance, C. and Campo, G. P.: A practical guide to wavelet analysis, *B. Am. Meteorol. Soc.*, 79, 61–78, 1998.
- Villani, M. G., Schmid, H. P., Su, H.-B., Hutton, J. L., and Vogel, C. S.: Turbulence statistics measurements in a northern hardwood forest, *Bound.-Lay. Meteorol.*, 108, 343–364, 2003.
- Wells, B. E.: *Atmospheric boundary layer bursting: the fundamental mechanism of particle entrainment*, Mechanical Engineering, Pullman, Washington State University, 80 pp., 1998.
- Wolfe, G. M., Thornton, J. A., Bouvier-Brown, N. C., Goldstein, A. H., Park, J.-H., McKay, M., Matross, D. M., Mao, J., Brune, W. H., LaFranchi, B. W., Browne, E. C., Min, K.-E., Wooldridge, P. J., Cohen, R. C., Crouse, J. D., Faloona, I. C., Gilman, J. B., Kuster, W. C., de Gouw, J. A., Huisman, A., and Keutsch, F. N.: *The Chemistry of Atmosphere-Forest Exchange (CAFE)*

- Model – Part 2: Application to BEARPEX-2007 observations, *Atmos. Chem. Phys.*, 11, 1269–1294, doi:10.5194/acp-11-1269-2011, 2011.
- Yamada, T. and Mellor, G.: A simulation of the Wangara boundary layer data, *J. Atmos. Sci.*, 32, 2309–2329, 1975.
- Yue, W. S., Meneveau, C., Parlange, M. B., Zhu, W. H., van Hout, R., and Katz, J.: A comparative quadrant analysis of turbulence in a plant canopy, *Water Resour. Res.*, 43, doi:10.1029/2006WR005583, 2007.
- Zhu, W., van Hout, R., and Katz, J.: PIV measurements in the atmospheric boundary layer within and above a mature corn canopy. Part II: Quadrant-hole analysis, *J. Atmos. Sci.*, 64, 2825–2838, 2007.